Journal of Materials Chemistry C

Accepted Manuscript

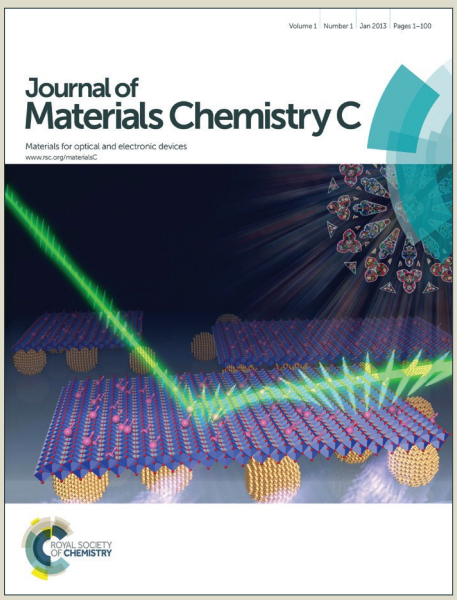

ROYAL SOCIETY OF CHEMISTRY

www.rsc.org/materialsC

Modular Synthetic Design Enables Precise Control of Shape and Doping in Colloidal Zinc Oxide Nanorods

*Saahil Mehra §, Emory M. Chan ||, Alberto Salleo §**

§ Department of Materials Science and Engineering, Stanford University, Stanford, California, 94305

|| The Molecular Foundry, Lawrence Berkeley National Laboratory, Berkeley, California, 94720

*Corresponding Author: *asalleo@stanford.edu*

ABSTRACT

Zinc oxide (ZnO) is a wide-band gap II-VI semiconductor with various optoelectronic applications owing to its transparency to visible light and tunable optical/electronic properties achieved by doping. While exquisite morphology control has been demonstrated for colloidal cadmium-chalcogenide II-VI nanocrystals over the past two decades, shape control strategies for solution-grown anisotropic ZnO nanocrystals (< 100 nm) are limited in scope - they suffer from large polydispersities and highly branched nanorods. Here, we present a modular synthetic design approach that overcomes many of the synthetic challenges associated with zinc oxide nanorods and enables nearly independent control of morphology and impurity incorporation. Manipulation of alcoholysis reaction kinetics through multiple precursor solution injections and judicious use of phosphonic acid surfactants enables the synthesis of nanorods with highly tunable shapes, lengths (40-200 nm), diameters (6-80nm), and doping levels (with aluminum - Al^{3+} - cations). This work will enable further studies on shape-dependent phenomena in colloidal metal oxide nanorods as well as facilitate understanding of doping and plasmonics in anisotropic nanoscale metal oxide systems.

INTRODUCTION

Control of the morphology and doping of semiconductor nanocrystals provides in principle a powerful platform for investigating shape- and composition-dependent nanoscale phenomena.[1-3] Remarkable control of size, shape, composition, and crystal structure can be achieved via colloidal syntheses for inorganic nanocrystals such as cadmium and lead chalcogenides, metals (gold, palladium, silver) and various metal oxide compositions.[3] Unfortunately, chemical strategies for imposing morphological and compositional control in colloidal nanocrystals are far from universal. For example, ZnO is a II-VI semiconductor like CdSe, but colloidal synthetic techniques to precisely specify the morphology and aliovalent doping of the more ionic ZnO at the sub-100 nanometer scale are lacking. This limited synthetic control has prevented the use of anisotropic ZnO nanocrystals in promising applications such as plasmonics,[4] spintronics,[5] electrochromics,[6] and photovoltaics.[7]

Here, we describe a non-aqueous, low-temperature colloidal synthetic approach for the growth of anisotropic ZnO nanocrystals with precise morphological control and broad dimensional tunability. The translation of surfactant-based shape control techniques optimized for CdSe to zinc oxide, a more ionic II-VI material, has only had limited success to date – typically, solution-grown ZnO nanostructures exhibit larger polydispersities and shape inhomogeneities than their CdSe counterparts.[8,9] Rod-like ZnO nanocrystals have previously been synthesized via hydrothermal,[10] oriented attachment,[11] and one-pot approaches.[9,12-16] A key limitation of these previous approaches is the inability to tune reaction parameters within those systems to control the morphology and dimensions of the nanorods. This lack of control in ZnO syntheses can partially be

attributed to unoptimized reaction chemistries which are less developed relative to cadmium chalcogenides - for example, in ZnO the strong ionic bond can trap defects during the growth process, thus resulting in high-energy sites that could drive the creation of branched morphologies.[17] As a result, research efforts are currently ongoing to provide an explanation of the growth mechanism and move towards rational syntheses of ZnO nanostructures.

To overcome this challenge, we have developed a modular synthetic design strategy that enables previously unrealized shape and doping control of colloidal ZnO rod-like nanocrystals**.** We demonstrate that temporal control of the concentrations of multiple reactants permits deterministic synthesis of ZnO nanorods with independently tunable lengths (40-110 nm), diameters (6-12 nm) and doping levels (with Al^{3+} cations). We devised this modular approach by separating each active component of the synthesis (metal precursor, dopant precursor, nucleophile, surfactant) into orthogonal precursor solutions and using an automated colloidal synthesis robot.[18] Unlike typical syringe pump or injection-based colloidal syntheses for oxide nanocrystals, this technique demonstrates for the first time that the selective addition of varying combinations and ratios of precursor solutions enables programmable control of reactant concentrations – and the resulting nanocrystal morphologies - throughout the course of a reaction.

Typically, colloidal metal oxide nanocrystal syntheses use a nucleophile (a fatty alcohol or amine) to convert the metal precursor into the active monomeric species via well-known alcoholysis or aminolysis routes.[2,9,19] Previous approaches to zinc oxide nanorods based on aminolysis[20,21] routes are limited to larger length scales (hundreds of nanometers) and branched morphologies due to growth from a common baseplate.[14-16,22]

Supersaturation of the active monomer drives the nucleation/growth processes, and the shapes/sizes can be modulated by the presence of surfactant molecules.[17] The synthetic reaction space for colloidal nanocrystals has many variables, including precursor/surfactant choices, reaction mechanism, temperature, precursor ratios, relative precursor addition rates (for injection syntheses), temperature, and time. To date, most syntheses of metal oxide nanocrystals have been limited to one-pot or single-injection approaches in which the temporal evolution of the individual precursor concentrations varies uncontrollably due to reactant consumption by nucleation and growth processes.

The method of multiple injections or, more broadly, sustained monomer concentration has been employed successfully for cadmium chalcogenide,[23-25] zinc selenide,[26] titanium dioxide,[20,21,27] and metal phosphide[28] nanorods. However, the attainable size ranges of these approaches are inherently limited since the continuous injection of one or two precursors eventually exhausts the availability of remaining reactants. By continuously injecting only a single precursor solution (or constant precursor ratio determined by the injection solution), the set of reaction conditions capable of being sampled is limited in scope. While sustained-growth approaches that alternate additions of reactive precursors exist for isotropic core-shell nanoparticles,[29] these techniques have not been adapted to synthesize much larger nanorods that would require many more injections. Our results show for the first time the success of this multiple injection approach to access nanoparticle geometries and compositions in zinc oxide not previously demonstrated in other ZnO syntheses.

RESULTS AND DISCUSSION

Length Control of Zinc Oxide Nanorods

We hypothesized that the growth of colloidal ZnO nanorods with tunable diameters and lengths could be achieved by a scheme (Figure 1A) in which the temporal variations of each reactant concentration were precisely tuned by repeatedly injecting sets of reagent solutions (metal precursor, surfactant, and nucleophile). Due to the large number of injections required by this strategy, we performed this scheme in an automated nanocrystal synthesis robot capable of precisely controlling the temperature profiles and precursor solution injection rates. We controlled the nanorod lengths by varying the number of injection sets, the diameters by tuning the temperature and initial surfactant (TDPA) concentration, and nanorod morphology by including TDPA in each injection set.

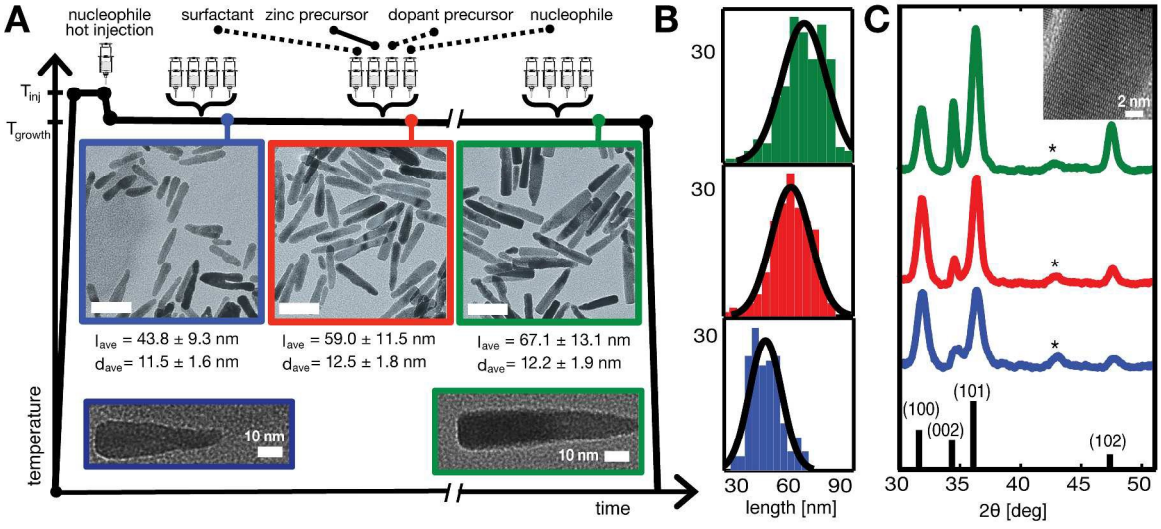

Figure 1. Morphological evolution of ZnO nanorods with multiple injections. TEM micrographs and process/temperature flow (A), size distribution histograms (B), and X-ray diffraction (XRD) patterns (C) of ZnO nanorods after 5 (blue), 10 (red), and 20 (green) injection sets. Injection sets consist of a series of precursor solutions added in different molar ratios at precise intervals. For this example, injection sets were only the

zinc precursor solution (solid line). All scale bars 50 nm. Reference pattern for wurtzite ZnO is shown. Asterisk on XRD plot indicates substrate peak.

ZnO nanorods synthesized using this scheme increased in length with increasing number of injection sets comprised of only the zinc acetate stock solution **(**Figure 1). The nanorods are single crystalline, as shown by high-resolution TEM characterization (Figure 1C, inset), and thus the relative XRD peak widths/intensities can be useful indicators of the change in dimension as a function of synthesis time. It is striking that the increases in length observed in the nanorods between the 5^{th} and 10^{th} injection sets (3 nm per injection set, 15 nm total) are significantly more than the increases observed between the 10^{th} and 20^{th} injection sets (0.8 nm per injection set, 8 nm total). This evidence suggests that the nucleophile concentration may be a limiting factor in the nucleation and growth process of the nanorods. Since the injection sets consisted only of the zinc acetate stock solution (the fatty alcohol is not replenished throughout the reaction), the initial oleyl alcohol concentration is progressively depleted. This results in a lower nanocrystal yield due to a limited number of nuclei and a slower growth reaction due to continuously decreasing availability of active monomer (which is produced by oleyl alcohol).

Seeking to maintain the nucleophile concentration levels, we added an additional module, oleyl alcohol, to our injection sets. Tests performed with increasing oleyl alcohol amounts per injection set resulted in significantly larger (6-10X) yields and similar nanorod dimensions, thus lending support to the claim that both oleyl alcohol and zinc acetate need to be present in the reaction mixture to maximize the number of initial

nuclei and facilitate the nanocrystal growth reaction. (Supplementary Information, Figure S3B)

The average nanorod diameters **(**Figure 1**)** vary minimally from 11.5 to 12.5 nm throughout the synthesis, indicating that growth of the nanorods during injection sets occurs almost exclusively in the axial direction. This evidence is further supported by XRD data (Figure 1C) that indicates increasing (002) peak intensities, decreasing peak widths, and nearly constant radial (100) peak widths as the number of injection sets increases. These data are consistent with elongation along the axial direction while the nanorod radii remain constant. Similar to the syntheses of Cd-chalcogenides, growth along the *c*-axis is expected due to the inherent surface energy anisotropy in wurtzite ZnO resulting from stacked Zn^{2+}/O^{2-} planes and the action of TDPA to passivate radial crystal facets.[3,30]

The nanorods grown by injecting only the zinc acetate solution (Figure 1) exhibit a distinct tapering of the diameters along the growth axis. Similar to syntheses for Cd-chalcogenide nanorods, we suggest that the presence of TDPA directs growth by stabilizing cation-terminated (001) faces. The high-energy (001) facets of wurtzite II-VI crystal structures are often eliminated during growth, resulting in a tapered morphology unless they are effectively passivated by a surfactant.[25] At the same time, the high surface energies of the (001) crystallographic facets explain their fast growth at high monomer concentrations (reaction-limited growth), since the growth reaction depends exponentially on the surface energy in this growth regime.[3,31] As the zinc acetate stock solution is injected during growth, the ratio of TDPA:Zn in the reaction bath continuously decreases, resulting in less available surfactant per unit surface area and increasingly

tapered pyramidal-type shapes. (Figure 2) As a result, we hypothesized that optimum alkylphosphonic acid concentration levels exist where the nanorod tapering would be controlled by surfactant stabilization of high surface energy facets and the reaction-limited growth regime would be maintained so anisotropic growth could still occur.

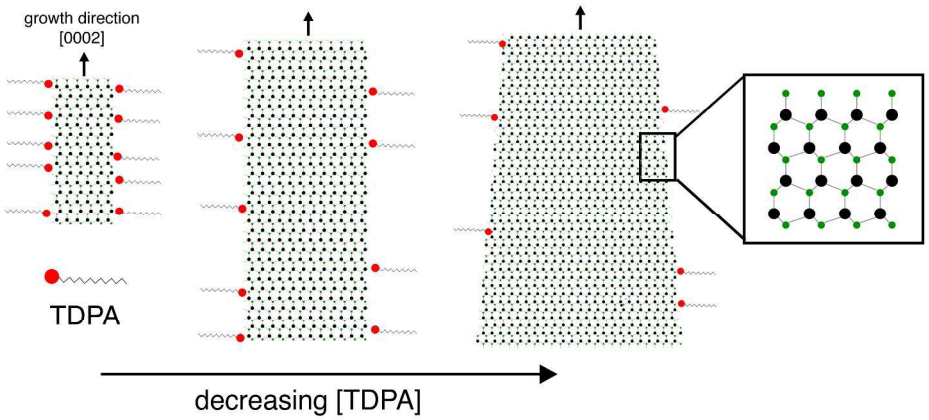

Figure 2: Schematic of nanorod shape evolution as a function of phosphonic acid (TDPA) concentration. Lower TDPA:Zn molar ratios result in tapered shapes due and larger diameters due to poor surface passivation.

Shape Control of Zinc Oxide Nanorods

To test this theory, we added a third injection module, TDPA, to the injection sets and maintained the TDPA:Zn molar ratio between 0.5:1 and 0.6:1 in the overall synthesis. Using repeated injection sets of the zinc acetate, oleyl alcohol, and TDPA modules, the shapes of the nanorods evolved from tapered rods (Figure 1) to cylindrical rods (Figure 3), indicating that the presence of TDPA acts as a stabilizing agent for high-energy surfaces. It is important to note that for TDPA:Zn molar ratios greater than 0.7:1, almost no nanocrystal yield was obtained since nucleation was almost entirely inhibited by the increased concentration of the less reactive zinc phosphonate precursor produced *in-situ* (Scheme 1, Reaction 1). These threshold TDPA:Zn molar ratios have been

similarly observed by others[8] and are notably lower than the ratios typically used for analogous Cd-chalcogenide nanorod syntheses (0.8-1:5:1 TDPA:Cd).[25,32] We further observed that when shorter alkylphosphonic acid chains (octylphosphonic acid) were used, the synthesized nanocrystals had tapered, pyramidal shapes due to less effective capping by the surfactant. This chain-length effect on tapering is likely a kinetic effect, as the binding energies of different chain length phosphonic acids to zinc are not expected to vary significantly with chain length.[33] We note that the effect of the shorter chain length is similar to the effects observed with low TDPA concentrations shown in Figure 1. (Supplementary Information, Figure S3D) On the other hand, when longer alkyl chains (octadecylphosphonic acid, ODPA) were used, almost all growth was inhibited due to the increased steric hindrance of the surfactant. Based on these observations, we chose to use TDPA due to its ability to effectively passivate nanocrystal surfaces without suppressing nanocrystal nucleation.

This tradeoff between nanocrystal yield and TDPA concentration is rationalized by considering the multiple roles surfactants play in nanocrystal syntheses. TDPA dynamically caps nanocrystal surfaces, participating in the equilibrium between the Zn-acetate precursor and the produced Zn-phosphonate, thereby creating a heterogeneous source of zinc monomers.[12] The increased stability of Zn-phosphonates compared to Cd-phosphonates results in a less reactive zinc precursor capable of precipitation during reactions (Zn^{2+} is harder than Cd^{2+} and phosphonate is a hard anion).[1,12,34,35] Thus, the use of large TDPA concentrations can inhibit nanocrystal nucleation from occurring, make it difficult to temporally separate nucleation and growth, and prevent the isolation of any nanocrystal yield. On the contrary, omission of TDPA during the synthesis resulted in

unconstrained growth of much larger nanoparticles with > 200 nm dimensions. The optimum ratios of TDPA:Zn throughout the reaction were thus chosen to maintain moderate growth rates in concert with morphology control.

The nanorods shown in Figure 3A-B have average lengths (Figure 3F) limited only by the number of injection sets performed, which implies that the nanorod lengths could be extended at will simply by increasing the total number of injection sets. This ability is a unique advantage of this modular approach when compared to single-solution injection approaches - the concentration of each reagent is controlled throughout the synthesis, which enables a deterministic growth reaction. Decreasing the addition rates of the zinc acetate stock solution from 15 μmol/min (Figure 3A,B) to 5 μmol/min (Figure 3C) resulted in significantly enhanced elongation (l_{ave} =108 nm) of the nanorods. We hypothesize that the amplitude of concentration fluctuations decreased with slower addition rates during injection sets, likely resulting in less homogeneous nucleation and leaving more active monomer for the growth reaction of the nanorods.

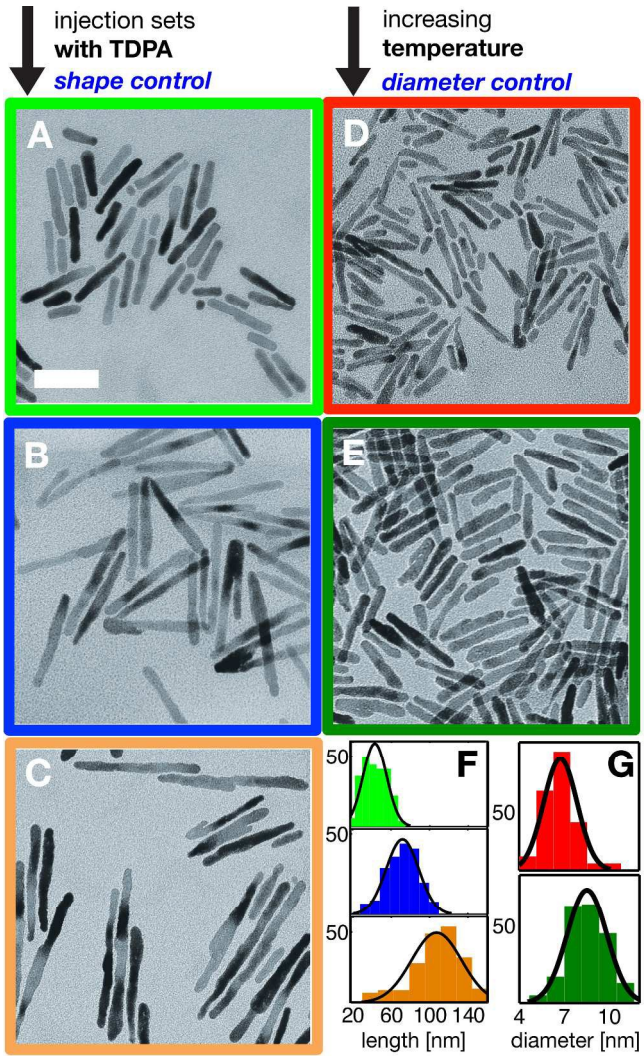

Figure 3. Shape control of ZnO nanorods. Length variation of nanorods achieved by using (A) 10 Injection Sets with TDPA (length: 42.6 +/- 12.4 nm), and (B) 25 Injection Sets with TDPA (length: 71.9 +/- 17.0 nm). Further length control achieved by (C) decreasing the injection rate by 3X (length: 107.2 +/- 26.1 nm). Diameter control accomplished by controlling injection/growth temperatures from (D) 255/235 °C (diameter: 6.8 +/- 1.1 nm) to (E) 285/265 °C (diameter: 8.5 +/- 1.3 nm). Length histograms for A-C are shown in (F), and diameter histograms for D and E are shown in (G). Scale bar is 50 nm for all images.

Diameter Control of Zinc Oxide Nanorods

We sought to control the nanorod diameters by varying the TDPA concentration and the temperature. The nanorod diameters in Figure 3 A-C decreased significantly to 8 nm when the molar ratios of TDPA:Zn in the overall synthesis were increased to 0.5-0.6:1 TDPA:Zn (compared to < 0.1:1 TDPA:Zn in Figure 3-1). The higher phosphonic acid concentration resulted in more effective capping of nanocrystal nuclei and smaller resulting nanorod diameters, which is consistent with control experiments showing smaller rod-like nanocrystal diameters for increased concentration of octylphosphonic acid in the synthesis (Figure 3D). For a given phosphonic acid concentration profile (determined by the injection set molar ratios), the diameters grow larger (from 6.8 to 8.5 nm**)** with increasing injection temperatures from 255 °C (Figure 3D) to 285 °C (Figure 3E). A similar trend was observed by Buonsanti et al. to achieve diameter control of colloidal Al:ZnO nanoparticles using carboxylic acid surfactants.[36] We explain this trend on the basis of the stability of the zinc phosphonate precursor, which likely results in poor temporal separation of the nucleation and growth processes: the large kinetic barrier to thermal activation of the zinc phosphonate bond results in slow monomer production . As a result, the thermal activation of the monomer production at higher temperatures results in simultaneous formation and growth of nuclei as well as elongation of nanocrystals. This hypothesis is confirmed by noting that nanocrystal yield and diameter both increase with temperature, which implies that at higher temperatures more nuclei are produced and more growth occurs. This behavior contrasts with the synthesis of anisotropic Cd-chalcogenides, which are performed at much higher temperatures (>300 °C). Unlike the stable Zn-phosphonate bond, the less stable cadmium phosphonate bond is easily

activated, which enables a distinct temporal separation of CdSe nucleation and growth stages.[3]

We note that the average nanorod diameters in Figure 3A-C are 8.2-8.6 nm, a strong indication that the injection set process uniquely modulates the nanorod length and minimal radial growth occurs during the synthesis. However, at low temperatures the thinner nanorods also exhibit surface inhomogeneities and branched morphologies, which can be explained by noting that ambient thermal energy at lower reaction temperatures is likely insufficient to anneal any defects that form out of the nanocrystals. This condition can result in the creation high-energy, defective nuclei and the growth of aggregated, branched nanostructures. Thus, while temperature does offer a route to controlling the diameter of these nanorods, the unintended morphological effects caused limit the usefulness of varying reaction temperature for this synthetic approach.

To achieve complete shape control of the nanorods and tunable diameters, we sought to control the radial dimension by tuning the concentration of TDPA and the relative TDPA:Zn molar ratio throughout the synthesis. Since phosphonic acids have been empirically shown to passivate radial faces – (100), (101) - in other wurtzite II-VI chalcogenides (CdTe, CdSe, CdS), we hypothesized that varying the relative concentration of the phosphonic acid over the duration of the synthesis could offer a more controllable route to diameter tunability. Figure 4 shows the results obtained for nanorods synthesized with various molar ratios of TDPA to Zn throughout the synthesis. In each synthesis, a particular molar ratio of TDPA to Zn (for example, 50%) was selected and maintained throughout all of the injection sets during the reaction.

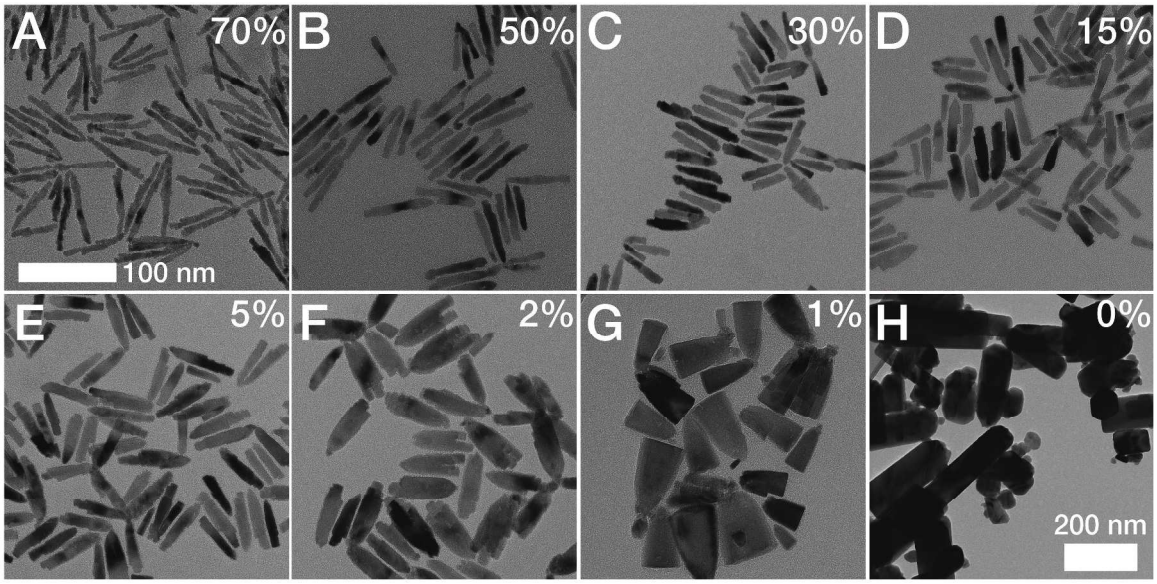

Figure 4: Nanorod morphologies as a function of decreasing TDPA:Zn molar ratio. Molar ratio in the synthesis varied from 70% (A), 50% (B), 30% (C), 15% (D), 5% (E), 2% (F), 1% (G), to 0% (H). Percentages are expressed as overall mol. % TDPA relative to Zn in the synthesis. For each synthesis, once the TDPA:Zn molar ratio was chosen it was maintained as constant throughout the reaction. Scale bars for A-G are all the same, 100 nm.

As the concentration of TDPA decreases the nanorod diameters increase more than an order of magnitude in dimension from < 8 nm (70% TDPA, Figure 4A) to > 80 nm (0% TDPA, Figure 4H). At very low surfactant concentrations, the nanorods begin growing as aggregated structures and form elongated, tapered pyramid-like morphologies. When no phosphonic acid is present, anisotropic macroparticles are obtained with highly polydisperse size distributions. This observation further elucidates the key role that surfactants play in modulating the growth process, slowing down the reaction kinetics, and minimizing the morphological effects that result from temperature fluctuations or concentration inhomogeneities in the reaction bath. The elongated pyramidal structures obtained at low surfactant concentrations resemble nanopyramid morphologies that are commonly achieved with solution-based ZnO syntheses. The low

surfactant concentrations result in poor capping of the high-surface energy (002) facets in addition to poor radial surface passivation, and as a result the crystal grows to minimized relative surface area of the high energy facets and the overall crystal free energy.

By varying the TDPA concentration in the synthesis, nanorods with tunable diameters over an order of magnitude are achieved (Supplementary Information, Figure S3F). The critical role of the phosphonic acid in modulating the growth of these nanocrystals is further shown by examining the relative diameters of the nanorods grown with no TDPA and 1% TDPA in synthesis. Interestingly, the role of TDPA in tuning the diameter at low surfactant concentration is highly non-linear. For example, the synthesis performed with 1% TDPA shows nanorod diameters less than half the size of the control experiment with no TDPA in the synthesis. The sensitivity of the reaction and resulting nanorod morphology to the presence of extremely low concentrations of TDPA demonstrates the critical role the surfactants play in determining the reaction mechanism and synthetic outcome.

Mechanistic Discussion

The surfactant concentration and nucleophile choices have been shown to play a critical role in determining the nanocrystal size and morphology. In addition, various reaction pathways can exist for the production of ZnO nanocrystals in this system based on the surfactant and nucleophile chemistry. The general reaction mechanism is described in Scheme 1 and relies on the alcoholysis of the heterogeneous precursor mixture of zinc acetate and zinc tetradecylphosphonate to produce the reactive zinc hydroxide monomer. This reaction mechanism (Scheme 1) has been established by others which synthesized nanopyramidal morphologies,[9,12,36-38] but anisotropic nanorod shapes require a more

complex reaction system to stabilize high-surface energy facets that typically would not exist and result in tapered, pyramidal nanoparticle shapes. The condensation of the zinc hydroxide monomers creates the Zn-O bonds that result in the homogeneous nucleation reaction or growth reaction, both of which are modulated by the surfactant chemistry.[12] The relative interplay between all these factors has a determining effect on the morphological outcome of the synthesis. Specifically, Tienes and co-workers showed that *in-situ* production of zinc phosphonate precursors from carboxylate salts enabled the growth of polydisperse, rod-like nanocrystals through an alcoholysis reaction.[12] The heterogeneous precursor mixture of zinc phosphonates and zinc acetate was shown to be critical for anisotropic growth to occur.

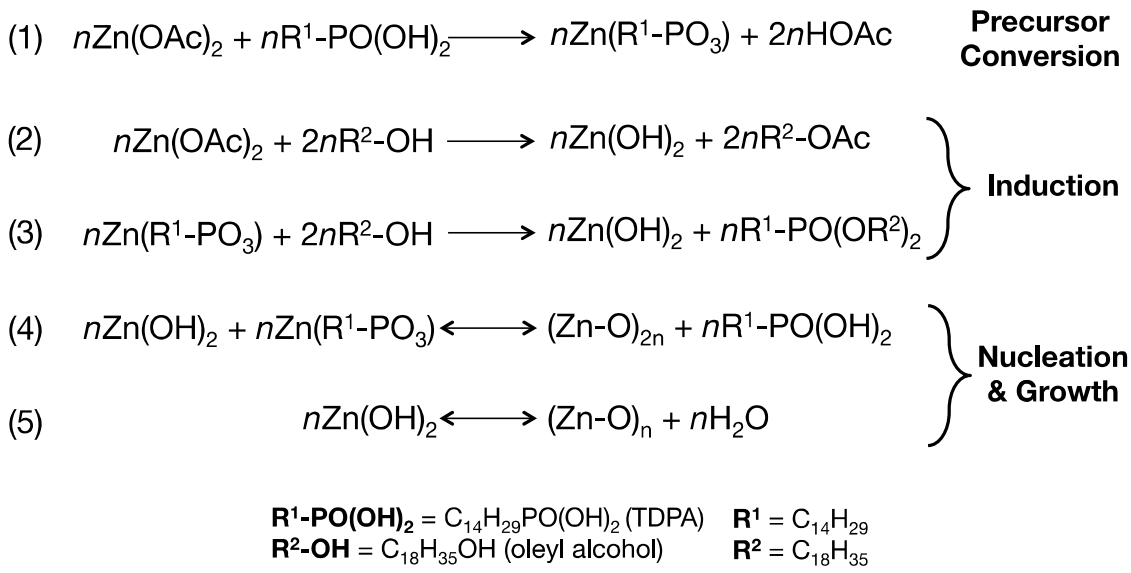

Scheme 1: **Generalized chemical reactions for growth of ZnO nanorods.** Reaction between the zinc precursor, alcohol, phosphonic acid resulting in precursor conversion, production of the active zinc hydroxide monomer (induction), and the nucleation/growth process.

Induction of the zinc hydroxide monomer to create a supersaturated precursor mixture is dependent on the relative monomer production rates from the mixture of heterogeneous precursor zinc salts (Scheme 1, Reactions 2/3). The subsequent nucleation and growth process occurs upon supersaturation of the zinc hydroxide monomer, and the monomers can produce water as a by-product (which evaporates) or regenerate the phosphonic acid surfactant Scheme 1, Reactions 4/5. The regenerated surfactant dynamically caps the crystal facets, and the growth process is based on competitive adsorption for a reactive site between the surfactant and Zn-O monomers.[12] The location of the Zn-O bond on the nanocrystal depends on the reactivity of different ZnO surfaces (correlated with surface energy) as well as the surface passivation by surfactants in the reaction mixture.

Aliovalent Doping of Zinc Oxide Nanorods

The precise control exhibited over the reaction chemistry enables the synthesis of size-controlled ZnO nanorods, and the versatility of this modular design approach enables the facile addition of aliovalent dopants via the incorporation of dopant modules into the injection sets. When aluminum acetylacetonate was incorporated in 9 and 15 molar percent (vs. Zn) into the ZnO synthesis (Figure 5), a progressive blueshift in the localized surface plasmon resonance absorption onset occurred, indicating an increased presence of free electrons. Elemental analysis measurements via ICP-AES confirm dopant incorporation in both the 9% Al-doped (1.0% atomic) and 15% Al-doped (1.6% atomic) cases. We note that the Al and Zn precursors are not balanced in chemical reactivities - Al^{3+} is a harder Lewis acid than Zn^{2+}, but the coordinating ligands are similarly hard anions, suggesting that the Al precursor will be less reactive than the Zn precursor. As a

result, a low Al^{3+} dopant incorporation rate is observed (roughly 10% of the initial feed ratio).[1] Higher dopant incorporation rates could be achieved by using longer chain, slower reacting zinc carboxylate precursors to promote Al incorporation. However, this comes at the expense of morphology control since the use of longer chain zinc carboxylates results in the synthesis of highly branched, tree-like nanoparticles (Supplementary Information, Figure S3E). The low incorporation rate achieved with Al-doping is the result of a trade-off between dopant incorporation and shape control in this reaction system. Although dopant induced shape effects have been previously reported in other nanocrystal systems,[38-40] our continuous precursor addition approach enables reaction-limited, anisotropic nanorod growth, thus allowing for simultaneous control of the shape and doping in these nanorods. The ability to tune the dopant introduction throughout the course of the reaction could enable the realization of completely independent shape control and dopant incorporation in colloidal zinc oxide nanorods – undoped ZnO nanorod seeds could be grown to preserve the shape, for example, and then the dopant could subsequently be added to introduce free carriers.

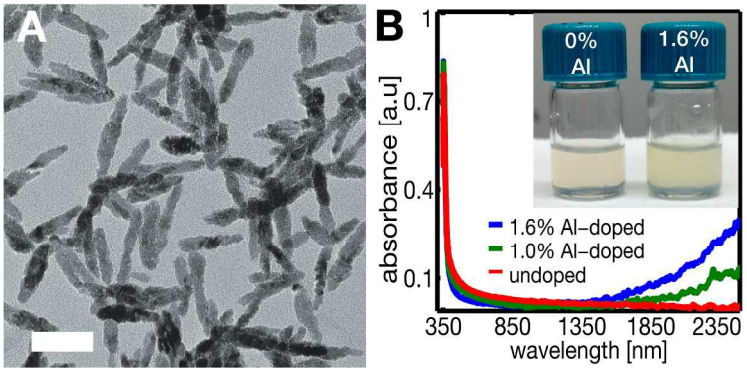

Figure 5. Characterization of Al-doped ZnO nanorods. TEM image (A) of 9% (synth) Al-doped ZnO nanorods, absorption spectra (B) of undoped/Al-doped nanorods (effective concentration) and photo of doped ZnO nanorod solution (inset). Scale bar is 50 nm.

EXPERIMENTAL

Apparatus. All nanocrystal syntheses performed in this work were performed at the Molecular Foundry using an automated nanocrystal synthesis robot, WANDA.[18] The development and characterization of relationships between reaction parameters and nanocrystal synthetic outcomes is complex and work-intensive due to the large parameter space of process variables associated with nanocrystal growth reactions. Using WANDA, a typically synthetic workflow to test and map the parameter space for a new synthesis involves reaction design, pre-reaction set-up in WANDA, performing the reaction, post-reaction work-up and characterization, and data analysis. This automated nanocrystal synthetic apparatus is capable of injecting multiple solutions over time into a reaction bath, thus enabling studies on nanocrystal synthesis reaction kinetics that are not typically achievable using single component multiple injection syntheses.

We show that for the case of colloidal zinc oxide nanorods one of the critical parameters is variation of the molar ratios of different reactants over time. The ability of the robot to effectively handle and dispense liquids enables typical flask-reaction actions, such as multiple injections or sampling aliquots, to be similarly performed by WANDA. Most importantly, the use of WANDA enables the reactant concentrations of multiple reactants to be simultaneously controlled as a function of reaction time with levels of precision and tunability not achievable by manual flask syntheses. By experimenting with this using WANDA, the optimal synthetic conditions for achieving reaction-limited growth for zinc oxide nanorods is achieved.

Chemicals. All chemicals were used as received. Oleyl alcohol (OlAlc) technical grade (85%), 1,12-dodecanediol (DDD), zinc acetate (ZnAc) dihydrate 99.999% (trace metals

basis), aluminum acetylacetonate (Alacac) 99% ReagentPlus, diphenyl ether (DPE), dioctyl ether (DOE), and octylamine (OctAm) were purchased from Sigma Aldrich. Tetradecylphosphonic Acid (TDPA) was purchased from PCI Synthesis. Trioctylphosphine Oxide 99% (TOPO) was purchased from STREM Chemicals. Nonanoic Acid (NonAc) was purchased from Alfa-Aesar. OlAlc and DOE were degassed under vacuum on a Schlenk line for 2 hours at 140 °C and subsequently transferred to a nitrogen glove box. The details of stock solution fabrication, the molar amounts of reactants used in each synthesis, the washing procedure used, and the characterization details are all provided in the Supplementary Information.

Synthesis. In a typical reaction, the robot initiated nucleation by injecting either the nucleophile (oleyl alcohol) or the zinc precursor (zinc acetate) into a reaction mixture held between 250-285 °C. The reaction bath consisted of surfactants (TDPA and trioctylphosphine oxide), solvent (dioctyl ether), and zinc acetate or fatty alcohol, respectively. To elongate the nanorods, a predetermined number (typically between 10-30) of injection sets consisting of sequentially added precursor stock solutions was performed in specified time intervals (usually 5 minutes) at the growth temperature (235-265 °C), T_{growth}. Joo et al. and Tienes et al. have used similar precursors to synthesize rod-like ZnO using a one-pot approach,[9,12] but in our case the separation of reactants into individual component solutions enabled a systematic optimization of the nanorod morphology, yield, and doping. The synthetic details, washing information, and characterization methods used are all described in detail in the Supporting Information.

CONCLUSIONS

ZnO nanorods were deterministically synthesized with excellent control over the length, diameter, shape, and doping level. This modular approach to colloidal synthesis enables interrogation of reaction conditions that are not typically accessible using one-pot or single-component injection approaches, thus enabling systematic studies of size-dependent properties of anisotropic zinc oxide nanocrystals. We expect that this synthetic design methodology will be generally applied to other materials systems and will facilitate the realization of new shape dependent plasmonic modes in anisotropic doped oxide nanostructures. Finally, we anticipate that the flexibility of this strategy will enable the fabrication of complex nanocrystal architectures such as axially modulated nanorod doping profiles for electronic applications where spatial impurity control is imperative.[41]

ACKNOWLEDGEMENTS

The authors gratefully acknowledge Dr. R. Buonsanti, Prof.. D. Milliron, A. Bergerud and E. Runnerstrom for helpful discussions and the National Science Foundation (Award No. DMR1007886) for financial support. All experiments were performed as part of the Molecular Foundry User Program, supported by the Office of Science, Office of Basic Energy Sciences, of the U.S. Department of Energy under Contract No. DE-AC02-05CH11231.

REFERENCES

1. Buonsanti, R. & Milliron, D. J. Chemistry of Doped Colloidal Nanocrystals. *Chem. Mater.* **25**, 1305-1317, (2013).
2. Jun, Y.-W., Choi, J.-S. & Cheon, J. Shape Control of Semiconductor and Metal Oxide Nanocrystals through Nonhydrolytic Colloidal Routes. *Angew. Chem. Int. Ed.* **45**, 3414-3439, (2006).
3. Yin, Y. & Alivisatos, A. P. Colloidal nanocrystal synthesis and the organic-inorganic interface. *Nature* **437**, 664-670, (2005).
4. Naik, G. V., Shalaev, V. M. & Boltasseva, A. Alternative Plasmonic Materials: Beyond Gold and Silver. *Adv. Mater.* **25**, 3264-3294, (2013).
5. Ogale, S. B. Dilute Doping, Defects, and Ferromagnetism in Metal Oxide Systems. *Adv. Mater.* **22**, 3125-3155, (2010).
6. Garcia, G., Buonsanti, R., Llordes, A., Runnerstrom, E. L., Bergerud, A. & Milliron, D. J. Near-Infrared Spectrally Selective Plasmonic Electrochromic Thin Films. *Advanced Optical Materials* **1**, 215-220, (2013).
7. Ellmer, K. & Klein, A. in *Transparent Conductive Zinc Oxide* Vol. 104 *Springer Series in Materials Science* (eds Klaus Ellmer, Andreas Klein, & Bernd Rech) (Springer-Verlag, 2008).
8. Cozzoli, P. D., Curri, M. L., Agostiano, A., Leo, G. & Lomascolo, M. ZnO Nanocrystals by a Non-hydrolytic Route: Synthesis and Characterization. *The Journal of Physical Chemistry B* **107**, 4756-4762, (2003).
9. Joo, J., Kwon, S. G., Yu, J. H. & Hyeon, T. Synthesis of ZnO Nanocrystals with Cone, Hexagonal Cone, and Rod Shapes via Non-Hydrolytic Ester Elimination Sol–Gel Reactions. *Adv. Mater.* **17**, 1873-1877, (2005).
10. Sun, B. & Sirringhaus, H. Solution-Processed Zinc Oxide Field-Effect Transistors Based on Self-Assembly of Colloidal Nanorods. *Nano Lett.* **5**, 2408-2413, (2005).
11. Pacholski, C., Kornowski, A. & Weller, H. Self-Assembly of ZnO: From Nanodots to Nanorods. *Angew. Chem. Int. Ed.* **41**, 1188-1191, (2002).

REFERENCES

12. Tienes, B. M., Perkins, R. J., Shoemaker, R. K. & Dukovic, G. Layered Phosphonates in Colloidal Synthesis of Anisotropic ZnO Nanocrystals. *Chem. Mater.* **25**, 4321-4329, (2013).
13. Yin, M., Gu, Y., Kuskovsky, I. L., Andelman, T., Zhu, Y., Neumark, G. F. & O'Brien, S. Zinc Oxide Quantum Rods. *J. Am. Chem. Soc.* **126**, 6206-6207, (2004).
14. Goris, L., Noriega, R., Donovan, M., Jokisaari, J., Kusinski, G. & Salleo, A. Intrinsic and Doped Zinc Oxide Nanowires for Transparent Electrode Fabrication via Low-Temperature Solution Synthesis. *J. Electron. Mater.* **38**, 586-595, (2009).
15. Yuhas, B. D., Zitoun, D. O., Pauzauskie, P. J., He, R. & Yang, P. Transition-Metal Doped Zinc Oxide Nanowires. *Angew. Chem. Int. Ed.* **45**, 420-423, (2006).
16. Zhang, Z., Lu, M., Xu, H. & Chin, W.-S. Shape-Controlled Synthesis of Zinc Oxide: A Simple Method for the Preparation of Metal Oxide Nanocrystals in Non-aqueous Medium. *Chemistry – A European Journal* **13**, 632-638, (2007).
17. Niederberger, M. & Garnweitner, G. Organic Reaction Pathways in the Nonaqueous Synthesis of Metal Oxide Nanoparticles. *Chemistry – A European Journal* **12**, 7282-7302, (2006).
18. Chan, E. M., Xu, C., Mao, A. W., Han, G., Owen, J. S., Cohen, B. E. & Milliron, D. J. Reproducible, High-Throughput Synthesis of Colloidal Nanocrystals for Optimization in Multidimensional Parameter Space. *Nano Lett.* **10**, 1874-1885, (2010).
19. Zhang, Z., Zhong, X., Liu, S., Li, D. & Han, M. Aminolysis Route to Monodisperse Titania Nanorods with Tunable Aspect Ratio. *Angew. Chem. Int. Ed.* **44**, 3466-3470, (2005).
20. Zhang, Z., Zhong, X., Liu, S., Li, D. & Han, M. Aminolysis Route to Monodisperse Titania Nanorods with Tunable Aspect Ratio. *Angew. Chem.* **117**, 3532-3536, (2005).
21. Buonsanti, R., Grillo, V., Carlino, E., Giannini, C., Kipp, T., Cingolani, R. & Cozzoli, P. D. Nonhydrolytic Synthesis of High-Quality Anisotropically Shaped Brookite TiO2 Nanocrystals. *J. Am. Chem. Soc.* **130**, 11223-11233, (2008).

REFERENCES

22. Kostopoulou, A., Thétiot, F., Tsiaoussis, I., Androulidaki, M., Cozzoli, P. D. & Lappas, A. Colloidal Anisotropic ZnO–Fe@FexOy Nanoarchitectures with Interface-Mediated Exchange-Bias and Band-Edge Ultraviolet Fluorescence. *Chem. Mater.* **24**, 2722-2732, (2012).
23. Shieh, F., Saunders, A. E. & Korgel, B. A. General Shape Control of Colloidal CdS, CdSe, CdTe Quantum Rods and Quantum Rod Heterostructures. *The Journal of Physical Chemistry B* **109**, 8538-8542, (2005).
24. Milliron, D. J., Hughes, S. M., Cui, Y., Manna, L., Li, J., Wang, L.-W. & Paul Alivisatos, A. Colloidal nanocrystal heterostructures with linear and branched topology. *Nature* **430**, 190-195, (2004).
25. Peng, Z. A. & Peng, X. Mechanisms of the Shape Evolution of CdSe Nanocrystals. *J. Am. Chem. Soc.* **123**, 1389-1395, (2001).
26. Cozzoli, P. D., Manna, L., Curri, M. L., Kudera, S., Giannini, C., Striccoli, M. & Agostiano, A. Shape and Phase Control of Colloidal ZnSe Nanocrystals. *Chem. Mater.* **17**, 1296-1306, (2005).
27. Koo, B., Park, J., Kim, Y., Choi, S.-H., Sung, Y.-E. & Hyeon, T. Simultaneous Phase- and Size-Controlled Synthesis of TiO2 Nanorods via Non-Hydrolytic Sol,àíGel Reaction of Syringe Pump Delivered Precursors. *The Journal of Physical Chemistry B* **110**, 24318-24323, (2006).
28. Park, J., Koo, B., Yoon, K. Y., Hwang, Y., Kang, M., Park, J.-G. & Hyeon, T. Generalized Synthesis of Metal Phosphide Nanorods via Thermal Decomposition of Continuously Delivered Metal,àíPhosphine Complexes Using a Syringe Pump. *J. Am. Chem. Soc.* **127**, 8433-8440, (2005).
29. Li, J. J., Wang, Y. A., Guo, W., Keay, J. C., Mishima, T. D., Johnson, M. B. & Peng, X. Large-Scale Synthesis of Nearly Monodisperse CdSe/CdS Core/Shell Nanocrystals Using Air-Stable Reagents via Successive Ion Layer Adsorption and Reaction. *J. Am. Chem. Soc.* **125**, 12567-12575, (2003).
30. Greene, L. E., Yuhas, B. D., Law, M., Zitoun, D. & Yang, P. D. Solution-grown zinc oxide nanowires. *Inorg. Chem.* **45**, 7535-7543, (2006).
31. Park, J., Joo, J., Kwon, S. G., Jang, Y. & Hyeon, T. Synthesis of Monodisperse Spherical Nanocrystals. *Angew. Chem. Int. Ed.* **46**, 4630-4660, (2007).

REFERENCES

32. Carbone, L. *et al.* Synthesis and Micrometer-Scale Assembly of Colloidal CdSe/CdS Nanorods Prepared by a Seeded Growth Approach. *Nano Lett.* **7**, 2942-2950, (2007).
33. Wang, W., Banerjee, S., Jia, S., Steigerwald, M. L. & Herman, I. P. Ligand Control of Growth, Morphology, and Capping Structure of Colloidal CdSe Nanorods. *Chem. Mater.* **19**, 2573-2580, (2007).
34. Donega, C. d. M. Synthesis and properties of colloidal heteronanocrystals. *Chem. Soc. Rev.* **40**, 1512-1546, (2011).
35. Parr, R. G. & Pearson, R. G. Absolute hardness: companion parameter to absolute electronegativity. *J. Am. Chem. Soc.* **105**, 7512-7516, (1983).
36. Buonsanti, R., Llordes, A., Aloni, S., Helms, B. A. & Milliron, D. J. Tunable Infrared Absorption and Visible Transparency of Colloidal Aluminum-Doped Zinc Oxide Nanocrystals. *Nano Lett.* **11**, 4706-4710, (2011).
37. Della Gaspera, E., Chesman, A. S. R., van Embden, J. & Jasieniak, J. J. Non-injection Synthesis of Doped Zinc Oxide Plasmonic Nanocrystals. *ACS Nano* **8**, 9154-9163, (2014).
38. Della Gaspera, E. *et al.* Low-Temperature Processed Ga-Doped ZnO Coatings from Colloidal Inks. *J. Am. Chem. Soc.* **135**, 3439-3448, (2013).
39. Gordon, T. R., Paik, T., Klein, D. R., Naik, G. V., Caglayan, H., Boltasseva, A. & Murray, C. B. Shape-Dependent Plasmonic Response and Directed Self-Assembly in a New Semiconductor Building Block, Indium-Doped Cadmium Oxide (ICO). *Nano Lett.* **13**, 2857-2863, (2013).
40. Yang, Y., Jin, Y., He, H., Wang, Q., Tu, Y., Lu, H. & Ye, Z. Dopant-Induced Shape Evolution of Colloidal Nanocrystals: The Case of Zinc Oxide. *J. Am. Chem. Soc.* **132**, 13381-13394, (2010).
41. Yang, C., Zhong, Z. & Lieber, C. M. Encoding Electronic Properties by Synthesis of Axial Modulation-Doped Silicon Nanowires. *Science* **310**, 1304-1307, (2005).

TABLE OF CONTENTS ENTRY:

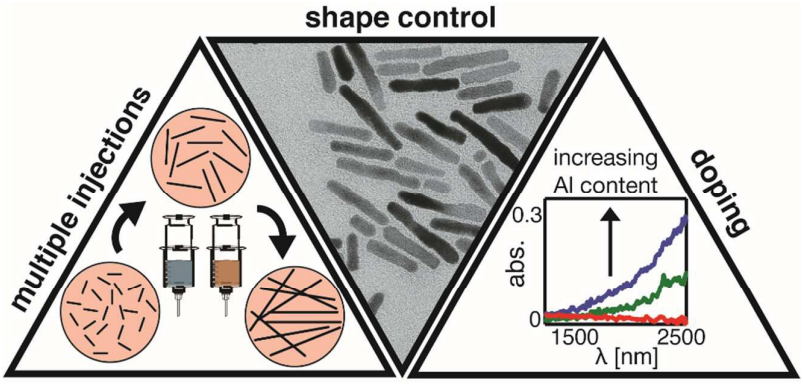

Highly tunable shapes and sizes of colloidal zinc oxide nanorods are achieved through a piecewise, multiple injection synthetic approach.